Theory of high-order harmonic generation in relativistic laser interaction with overdense plasma

T. Baeva,[1] S. Gordienko,[2] and A. Pukhov[1]
[1]*Institut für Theoretische Physik I, Heinrich-Heine-Universität Düsseldorf, D-40225 Dusseldorf, Germany*
[2]*L.D. Landau Institute for Theoretical Physics, Moscow, Russia*
(Received 28 April 2006; published 12 October 2006)

High-order harmonic generation due to the interaction of a short ultrarelativistic laser pulse with overdense plasma is studied analytically and numerically. On the basis of the ultrarelativistic similarity theory we show that the high-order harmonic spectrum is universal, i.e., it does not depend on the interaction details. The spectrum includes the power-law part $I_n \propto n^{-8/3}$ for $n < \sqrt{8\alpha}\gamma_{\max}^3$, followed by exponential decay. Here $\gamma_{\max}$ is the largest relativistic γ factor of the plasma surface and α is the second derivative of the surface velocity at this moment. The high-order harmonic cutoff at $\propto \gamma_{\max}^3$ is parametrically larger than the $4\gamma_{\max}^2$ predicted by the simple "oscillating mirror" model based on the Doppler effect. The cornerstone of our theory is the new physical phenomenon: spikes in the relativistic γ factor of the plasma surface. These spikes define the high-order harmonic spectrum and lead to attosecond pulses in the reflected radiation.

DOI: 10.1103/PhysRevE.74.046404 PACS number(s): 52.27.Ny, 42.65.Ky, 52.38.Ph

I. INTRODUCTION

High-order harmonic generation (HHG) from relativistically intense laser pulses interacting with solid targets has been identified as a promising way to generate bright ultrashort bursts of x rays [1–3] as well as a powerful tool for plasma diagnostics, already successfully applied for investigation of the strongest magnetic fields generated in a laboratory [4,5]. The power-law spectrum of the high-order harmonics generated at the boundary of overdense plasma was recently measured experimentally [6].

For the first time this spectacular phenomenon was observed with nanosecond pulses of long wavelength (10.6 μm) CO_2 laser light [8]. Shortly after the experimental observation in 1981, Bezzerides *et al.* studied the problem of harmonic light emission theoretically [9]. Their approach based on nonrelativistic equations of motion and hydrodynamic approximation for the plasma predicted a cutoff of the harmonic spectrum at the plasma frequency.

Ten years later, in 1993, a new approach to the interaction of an ultrashort, relativistically strong laser pulse with overdense plasma was proposed by Bulanov *et al.* [10]. They "interpreted the harmonic generation as due to the Doppler effect produced by a reflecting charge sheet, formed in a narrow region at the plasma boundary, oscillating under the action of the laser pulse" [10]. The "oscillating mirror" model predicts a cutoff harmonic number of $4\gamma_{\max}^2$, where $\gamma_{\max}$ is the maximal γ factor of the mirror.

At the beginning of 1996, numerical results of particle-in-cell simulations of the harmonic generation by femtosecond laser-solid interaction were presented by Gibbon [11]. He demonstrated numerically that the high harmonic spectrum goes well beyond the cutoff predicted in Ref. [9] and also presented a numerical fit for the spectrum, which approximated the intensity of the nth harmonic as $I_n \propto n^{-5}$. At about the same time, the laser-overdense plasma interaction was also studied by Lichters *et al.* [12].

The same year, the analytical work by von der Linde and Rzazewski [13] appeared. The authors used the oscillating mirror model and approximated the oscillatory motion of the mirror as a sine function of time without analysis of the applicability of this approximation. With the explicit form of the mirror motion an analytical formula for the harmonic spectrum was obtained.

In the weakly and moderately relativistic regime, when the laser intensity $I\lambda^2 \leqslant 10^{18}$ W μm^2/cm^2, the dynamics of the reflecting surface can also be influenced by harmonic resonances [14,15].

An attempt to describe analytically the high-order harmonics generated at the boundary of overdense plasma by a short ultraintense laser pulse in a universal way that does not rely on an explicit formula for the exact plasma mirror motion was made in Ref. [1]. This work proposed the idea of universality of the harmonic spectrum. Making use of the steepest descent method, the authors of Ref. [1] have shown that the harmonic spectrum follows a slowly decaying power law $I_n \propto n^{-p}$, where the exponent p was expected to be $p = 2.5$. The analytically predicted power-law spectrum has found a spectacular independent experimental confirmation in the recently published paper of Dromey *et al.* [6]. The experiment [6] confirmed the power-law spectrum decay down to the "water window" range that opens a way to a number of interesting potential applications [7].

In the present work we extend and generalize the physical results obtained in Ref. [1], present the detailed physical picture of the HHG, and consolidate the analytical approximations. For the last couple of years the interest in the process of HHG from plasmas has enjoyed a revival thanks to the increasing interest in attoscience. The recent impressive progress in the physics of attosecond x-ray pulses [16,17] triggers the fascinating question of whether a range of even shorter ones is achievable with the contemporary or developing experimental technology.

Plaja *et al.* [18] were the first to realize that the simple concept of the oscillating mirror gives an opportunity to produce extremely short pulses and presented a numerical proof that the radiation generated by oscillating plasma surfaces comes in the form of subfemtosecond pulses. For the first time the idea to use the plasma harmonics for the generation of subattosecond pulses (zeptosecond range) was announced in Ref. [1].

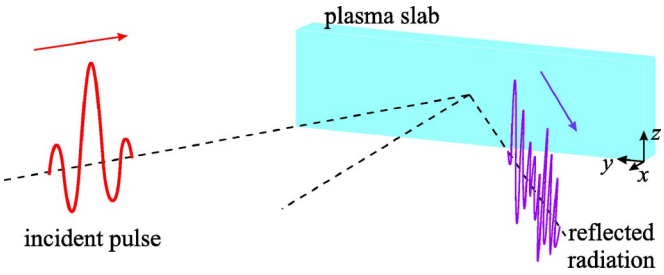

FIG. 1. (Color online) Geometry of the problem. The laser pulse is moving towards the overdense plasma slab, x is perpendicular to the surface, and y and z are parallel to it.

The present paper is based on the physical picture discussed already in Ref. [1]. Yet, it goes further and studies in detail the ultrarelativistic plasma-surface motion. We show that the high-order harmonics are generated due to sharp spikes in the relativistic γ factor of the plasma surface. This new physical phenomenon leads to the spectrum cutoff at the harmonic number n_{cutoff},

$$n_{\text{cutoff}} = \sqrt{8\alpha}\gamma_{\max}^3. \tag{1}$$

The cutoff (1) is much higher than the $4\gamma_{\max}^2$ cutoff predicted by the simple oscillating mirror model. Here $\gamma_{\max}$ is the maximum γ factor of the surface and α is a numerical factor of the order of unity, related to the plasma-surface acceleration. Explicit expressions for the attosecond pulse duration as a function of the laser-plasma parameters and the filter threshold are derived.

Our analysis significantly exploits the relativistic plasma-similarity theory [20,21], which was developed after Ref. [1] had been published. The similarity theory enables us to consolidate our previous results and to present them in a straightforward and clear way.

In this paper we first discuss the physical picture of HHG. The production of high-order harmonics is attributed to the new physical effect of the relativistic spikes. Then, we develop analytical theory describing the spectrum of the high-order harmonics and show that this spectrum is universal with slow power-law decay. Finally, the theory is compared with direct particle-in-cell (PIC) simulations.

II. PHYSICAL PICTURE OF HHG AT OVERDENSE PLASMA BOUNDARY

In this section we state the problem of HHG at the boundary of overdense plasma and qualitatively describe its main features, which will find their analytical and numerical confirmation in what follows.

Let us consider a short laser pulse of ultrarelativistic intensity, interacting with the sharp surface of an overdense plasma slab (see Fig. 1). We assume that the incident laser pulse is short, so that we can neglect the slow ion dynamics and consider the electron motion only. The electrons are driven by the laser-light pressure; a restoring electrostatic force comes from the ions. As a consequence, the plasma surface oscillates and the electrons gain a normal momentum component.

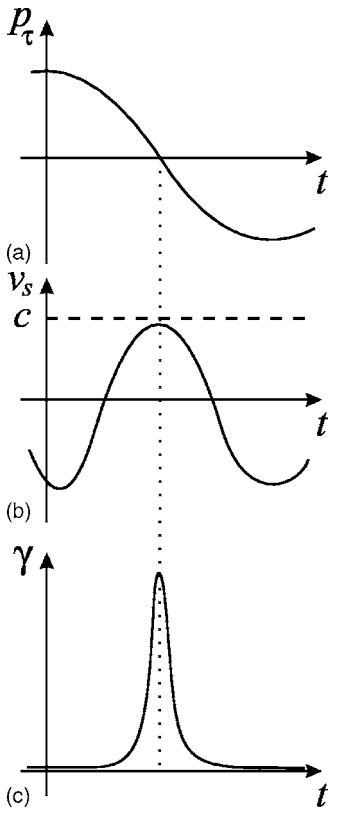

FIG. 2. (a) Electron momentum component parallel to the surface as a function of time. (b) The velocity of the plasma surface v_s is a smooth function of time, unlike the γ factor of the surface (c).

Since the plasma is overdense, the incident electromagnetic wave is not able to penetrate it. This means that there is an electric current along the plasma surface. For this reason, the momenta of electrons in the skin layer have, apart from the components normal to the plasma surface, also tangential components.

According to the relativistic similarity theory [21], both the normal and tangential components are of the order of the dimensionless electromagnetic potential a_0. Consequently, the actual electron momenta make a finite angle with the plasma surface most of the time.

Since we consider a laser pulse of ultrarelativistic intensity, the motion of the electrons is ultrarelativistic. In other words, their velocities are approximately c. Though the motion of the plasma surface is qualitatively different, its velocity v_s is not ultrarelativistic most of the time but smoothly approaches c only when the tangential electron momentum vanishes [see Fig. 2(b)].

The γ factor of the surface γ_s also shows specific behavior. It has sharp peaks at those times when the velocity of the surface approaches c [see Fig. 2(c)]. Thus, while the velocity function v_s is characterized by its smoothness, the distinctive features of γ_s are its quasisingularities.

When v_s reaches its maximum and γ_s has a sharp peak, high-order harmonics of the incident wave are generated and can be seen in the reflected radiation. Physically this means that the high-order harmonics are due to the collective motion of bunches of fast electrons moving towards the laser pulse [19].

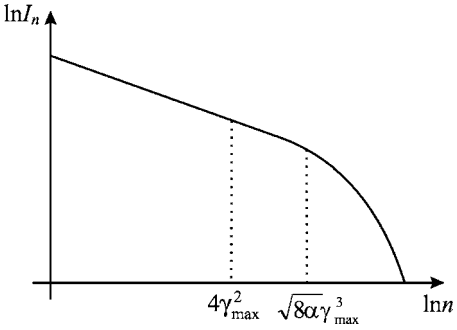

FIG. 3. The universal high-order harmonic spectrum contains power-law decay and exponential decay (plotted in a logarithmic scale).

These harmonics have two very important properties. First, their spectrum is universal. The exact motion of the plasma surface can be very complicated, since it is affected by the shape of the laser pulse and can differ for different plasmas. Yet the qualitative behavior of v_s and γ_s is universal, and since it governs the HHG, the spectrum of the high-order harmonics does not depend on the particular surface motion.

We show below that the high-order harmonic spectrum contains two qualitatively different parts: power-law decay and exponential decay (see Fig. 3). In the power-law part the spectrum decays as

$$I_n \propto 1/n^{8/3}, \tag{2}$$

up to a critical harmonics number that scales as γ^3_{max}, where I_n is the intensity of the nth harmonic (see Sec. V). Here γ_{max} is the maximal γ factor of the point, where the component of the electric field tangential to the surface vanishes (see Sec. IV).

The second important feature of the high-order harmonics is that they are phase locked. This observation is of particular value, since it allows for the generation of attosecond and even subattosecond pulses [1].

III. ULTRARELATIVISTIC SIMILARITY AND THE PLASMA-SURFACE MOTION

The analytical theory presented in this work is based on the similarity theory developed in Ref. [21] for collisionless ultrarelativistic laser-plasma regime and is valid both for under- and overdense plasmas. The ultrarelativistic similarity theory states that when the dimensionless laser vector potential $\mathbf{a}_0 = e\mathbf{A}_0/mc^2$ is large ($a_0^2 \gg 1$) the plasma-electron dynamics does not depend on a_0 and the plasma-electron density N_e separately. Instead they merge in the single dimensionless similarity parameter S defined by

$$S = \frac{N_e}{a_0 N_c}, \tag{3}$$

where $N_c = \omega_0^2 m/4\pi e^2$ is the critical electron density for the incident laser pulse with amplitude a_0 and carrier frequency ω_0.

In other words, when the plasma density N_e and the laser amplitude a_0 change simultaneously, so that $S = N_e/a_0 N_c$ = const, the laser-plasma dynamics remains similar. In particular, this basic ultrarelativistic similarity means that for different interactions with the same S=const, the plasma electrons move along similar trajectories while their momenta $\mathbf{p}$ scale as

$$\mathbf{p} \propto a_0. \tag{4}$$

The S similarity corresponds to a multiplicative transformation group of the Vlasov-Maxwell equations, which appears in the ultrarelativistic regime. The similarity is valid for arbitrary values of S. Physically the S parameter separates relativistically overdense plasmas ($S \gg 1$) from underdense ones ($S \ll 1$).

To apply the key result (4) of the similarity theory to the plasma-surface motion, we rewrite Eq. (4) for the electron momentum components that are perpendicular, $\mathbf{p}_n$, and tangential, $\mathbf{p}_\tau$, to the plasma surface;

$$\mathbf{p}_n \propto a_0, \quad \mathbf{p}_\tau \propto a_0. \tag{5}$$

This result is significant. It shows that when we increase the dimensionless vector potential a_0 of the incident wave while keeping the plasma overdense, so that S=const, both $\mathbf{p}_n$ and $\mathbf{p}_\tau$ grow as a_0. In other words the velocities of the skin-layer electrons

$$v = c\sqrt{\frac{\mathbf{p}_n^2 + \mathbf{p}_\tau^2}{m_e^2 c^2 + \mathbf{p}_n^2 + \mathbf{p}_\tau^2}} = c[1 - O(a_0^{-2})] \tag{6}$$

are about the speed of light almost at all times. Yet the relativistic γ factor of the plasma surface $\gamma_s(t')$ and its velocity $\beta_s(t')$ behave in a quite different way. To realize this key fact, let us consider the electrons at the very boundary of the plasma. The scalings (5) state that the momenta of these electrons can be represented as

$$\mathbf{p}_n(t') = a_0 \mathbf{P}_n(S, \omega_0 t'),$$

$$\mathbf{p}_\tau(t') = a_0 \mathbf{P}_\tau(S, \omega_0 t'), \tag{7}$$

where $\mathbf{P}_n$ and $\mathbf{P}_\tau$ are universal functions, which depend on the pulse shape and the S parameter rather than on a_0 or N_e separately. Consequently, for $\beta_s(t')$ and $\gamma_s(t')$ one obtains

$$\beta_s(t') = \frac{p_n(t')}{\sqrt{m_e^2 c^2 + \mathbf{p}_n^2(t') + \mathbf{p}_\tau^2(t')}} = \frac{P_n(t')}{\sqrt{\mathbf{P}_n^2(t') + \mathbf{P}_\tau^2(t')}} - O(a_0^{-2}), \tag{8}$$

$$\gamma_s(t') = \frac{1}{\sqrt{1 - \beta_s^2(t')}} = \sqrt{1 + \frac{\mathbf{P}_n^2(t')}{\mathbf{P}_\tau^2(t')}} + O(a_0^{-2}). \tag{9}$$

One sees from Eq. (6) that when a_0 gets large, the relativistic γ factor of the electrons becomes large too and their velocities approach the velocity of light. However, the dynamics of the plasma boundary is significantly different. For large a_0s the plasma-boundary motion does not enter the ultrarelativistic regime and its relativistic γ factor $\gamma_s(t')$ is generally of the order of unity. Yet there is one exception: if at the moment t'_g it happens that $\mathbf{P}_\tau(S, t'_g) = 0$, i.e.,

$$\mathbf{p}_\tau(S,t_g')=0, \tag{10}$$

we have

$$\gamma_s=\frac{1}{\sqrt{1-\beta_s^2}}=\sqrt{\frac{\mathbf{p}_n^2+m_e^2c^2}{m_e^2c^2}}\propto a_0. \tag{11}$$

So the relativistic γ factor of the boundary jumps to $\gamma_s(t_g')\propto a_0$ and the duration of the relativistic γ-factor spike can be estimated as

$$\Delta t'\propto 1/(a_0\omega_0). \tag{12}$$

For the velocity of the plasma boundary one finds analogously that it smoothly approaches the velocity of light as $\beta_s(t_g')=[1-O(a^{-2})]$. Figure 2 represents schematically this behavior. As we will see later, the γ_s spikes cause the generation of high-order harmonics in the form of ultrashort laser pulses.

IV. BOUNDARY CONDITION: ENERGY CONSERVATION AND THE APPARENT REFLECTION POINT

In this section we introduce the boundary condition describing the laser-overdense plasma interaction appealing to physical arguments, just as it was previously done in Refs. [1,18]. Mathematically rigorous analysis of the boundary condition is given in Ref. [19]. However, for the purposes of the present work it is sufficient to treat this problem on a more intuitive basis [1].

One might expect that the oscillating mirror model could describe the laser-plasma interaction in our problem. Therefore we want to explain in detail why it is not the case and then present the derivation of the correct boundary condition.

The oscillating mirror model implies that the tangential components of the vector potential are zero at the mirror surface. As a consequence, if the ideal mirror moves with $\gamma\gg 1$ towards the laser pulse with the electric field E_l and the duration τ_0, the reflected electric field will be $E_{\mathrm{refl}}\propto\gamma^2E_l$ and the pulse duration will be $\tau_{\mathrm{refl}}\propto\tau_0/\gamma^2$. The energy of the reflected pulse would then be γ^2 times higher than that of the incident one. However, since the plasma surface is driven by the same laser pulse, this scaling is energetically prohibited and consequently the plasma cannot be described as an "ideal mirror."

To derive the correct boundary condition, let us consider the tangential vector-potential components of a laser pulse normally incident onto an overdense plasma slab. These components satisfy the equation

$$\frac{1}{c^2}\frac{\partial^2\mathbf{A}_\tau(t,x)}{\partial t^2}-\frac{\partial^2\mathbf{A}_\tau(t,x)}{\partial x^2}=\frac{4\pi}{c}\mathbf{j}(t,x), \tag{13}$$

where $\mathbf{A}_\tau(t,x=-\infty)=0$ and $\mathbf{j}$ is the tangential plasma-current density. Equation (13) yields

$$\mathbf{A}_\tau(t,x)=2\pi\int_{-\infty}^{+\infty}\mathbf{J}(t,x,t',x')dt'dx'. \tag{14}$$

Here $\mathbf{J}(t,x,t',x')=\mathbf{j}(t',x')(\Theta_--\Theta_+)$, where we have defined $\Theta_-=\Theta(t-t'-|x-x'|/c)$ and $\Theta_+=\Theta[t-t'+(x-x')/c]$, using the Heaviside step function $\Theta(t)$. Due to this choice of $\mathbf{J}$ the vector potential $\mathbf{A}_\tau(t,x)$ satisfies both Eq. (13) and the boundary condition at $x=-\infty$ since $\mathbf{J}(t,x=-\infty,t',x')=0$. The tangential electric field is $\mathbf{E}_\tau=-(1/c)\partial_t\mathbf{A}_\tau(t,x)$. If we denote the position of the electron fluid surface by $X(t)$ we have

$$\mathbf{E}_\tau[t,X(t)]=\frac{2\pi}{c}\sum_{\alpha=-1}^{\alpha=+1}\alpha\int_0^{-\infty}\mathbf{j}[t+\alpha\xi/c,X(t)+\xi]d\xi, \tag{15}$$

where $\xi=x'-X(t)$.

Now one has to estimate the parameters characterizing the skin layer, i.e., the characteristic time τ_s of skin-layer evolution (in the comoving reference frame) and the skin-layer thickness δ. Since the plasma is driven by the light pressure, one expects that $\tau_s\propto 1/\omega_0$. The estimation of δ is more subtle. From the ultrarelativistic similarity theory follows that $\delta\propto(c/\omega_0)S^\Delta$, where $S\gg 1$ for strongly overdense plasmas and Δ is an exponent that has to be found analytically. In this work we do not discuss the exact value of Δ, but notice that this quantity does not depend on either S, or a_0. On the other hand, the denser the plasma, the less the value of δ. This condition demands that $\Delta<0$ and we get $c/\omega_0\gg\delta$ for $S\gg 1$.

If the characteristic time τ_s of the skin-layer evolution is long $(c\tau_s\gg\delta)$, then we can use the Taylor expansion $\mathbf{j}[t\pm\xi/c,x'=X(t)+\xi]\approx\mathbf{j}(t,x')\pm\boldsymbol{\epsilon}$, where $\boldsymbol{\epsilon}=(\xi/c)\partial_t\mathbf{j}(t,x')$, and substitute this expression into Eq. (15). The zero-order terms cancel each other and we get $\mathbf{E}_\tau[t,X(t)]\propto J_p(\delta/c\tau)\ll E_l$, where $J_p\propto cE_l$ is the maximum plasma-surface current. Thus, as long as the skin layer is thin and the plasma-surface current is limited, we can use the Leontovich boundary condition [22]

$$\mathbf{e}_n\times\mathbf{E}[t,X(t)]=0. \tag{16}$$

This condition has a straightforward relation to energy conservation. Indeed, if we consider the Poynting vector

$$\mathbf{S}=\frac{c}{4\pi}\mathbf{E}\times\mathbf{B}, \tag{17}$$

we notice that the boundary condition (16) represents a balance between the incoming and reflected electromagnetic energy flux at the boundary $X(t)$.

The boundary condition (16) allows for another interpretation. An external observer sees that the electromagnetic radiation gets reflected at the point $x_{\mathrm{ARP}}(t)$, where the normal component of the Poynting vector $\mathbf{S}_n=c\mathbf{E}_\tau\times\mathbf{B}_\tau/4\pi=0$, implied by $\mathbf{E}_\tau(x_{\mathrm{ARP}})=0$. We call the point $x_{\mathrm{ARP}}(t)$ *the apparent reflection point* (ARP).

The actual location of the ARP can be easily found from the electromagnetic-field distribution in front of the plasma surface. The incident laser field in vacuum runs in the negative x direction, $\mathbf{E}^i(x,t)=\mathbf{E}^i(x+ct)$, while the reflected field is translated backwards, $\mathbf{E}^r(x,t)=\mathbf{E}^r(x-ct)$. The tangential components of these fields interfere destructively at the ARP position $x_{\mathrm{ARP}}(t)$, so that the implicit equation for the apparent reflection point $x_{\mathrm{ARP}}(t)$ is

$$\mathbf{E}_\tau^i(x_{\mathrm{ARP}}+ct)+\mathbf{E}_\tau^r(x_{\mathrm{ARP}}-ct)=0. \tag{18}$$

We want to emphasize that Eq. (18) contains the electromagnetic fields in vacuum. That is why the reflection point x_{ARP} is *apparent*. The real interaction within the plasma skin layer can be very complex. Yet, an external observer, who has information about the radiation in vacuum only, sees that $\mathbf{E}_\tau=0$ at x_{ARP}. The ARP is located within the skin layer at the electron-fluid surface, which is much shorter than the laser wavelength for overdense plasmas for which the similarity parameter is $S\gg 1$. In this sense, the ARP is attached to the oscillating plasma surface.

V. HIGH-ORDER HARMONIC UNIVERSAL SPECTRUM

According to Eq. (16), the electric field of the reflected wave at the plasma surface is

$$\mathbf{E}_r[t',X(t')]=-\mathbf{E}_i[t',X(t')], \tag{19}$$

where $\mathbf{E}_i[t',X(t')]=-(1/c)\partial_{t'}\mathbf{A}_i[t',X(t')]$ is the incident laser field and t' is the reflection time. The one-dimensional wave equation translates signals in vacuum without change. Thus the reflected wave field at the observer position x and time t is $\mathbf{E}_r(t,x)=-\mathbf{E}_i[t',X(t')]$. Setting $x=0$ at the observer position we find that the Fourier spectrum of the electric field $\mathbf{E}_r(t,x=0)$ is

$$\mathbf{E}_r(\Omega)=\frac{m_e c\omega}{e\sqrt{2\pi}}\int_{-\infty}^{+\infty}\mathrm{Re}(i\mathbf{a}\{[ct'+X(t')]/c\tau_0\}\times\exp[-i\omega_0 t'-i\omega_0 X(t')/c)]\exp(-i\Omega t)dt, \tag{20}$$

where

$$t'-X(t')/c=t \tag{21}$$

is the retardation relation [12].

The fine structure of the spectrum of $\mathbf{E}_r(t)$ depends on the particular surface motion $X(t)$, which is defined by the complex laser-plasma interaction at the plasma surface. Previous theoretical works on high-order harmonic generation from plasma surfaces [11–13,18] tried to approximate the function $X(t)$ in order to evaluate the harmonic spectrum. The analytical description of the high-order harmonic intensity spectrum and the concept of universality were presented in Ref. [1]. This work has shown that the most important features of the high-order harmonic spectrum do not depend on the detailed structure of $X(t)$. The relativistic similarity theory, which was developed later [21] not only simplifies the physical picture of HHG, but, as we will see below, also influences the saddle-point technique [23] in this regime.

To find the spectrum, we notice that the investigation of $\mathbf{E}_r(\Omega)$ [Eq. (20)] is equivalent to the investigation of the function

$$f(n)=f_+(n)+f_-(n), \tag{22}$$

where

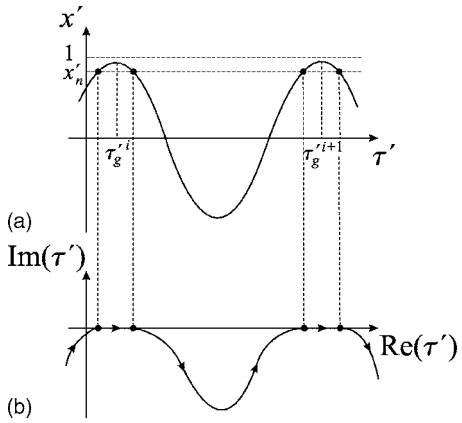

FIG. 4. Surface dynamics and path integration in Eq. (25). (a) Velocity $x'(\tau')$ of the plasma surface; $x'_n=(n-1)/(n+1)$ are the saddle points corresponding to $d\Theta/d\tau'=0$. (b) The integration path can be shifted below the real axis everywhere except in the neighborhood of τ'_g (dashed regions).

$$f_\pm=\pm\int_{-\infty}^{+\infty}\mathbf{g}[\tau'+x(\tau')]\exp\{\pm i[\tau'+x(\tau')]-in\tau\}d\tau. \tag{23}$$

Here $\tau=\omega_0 t$, $\tau'=\omega_0 t'$, $n=\Omega/\omega_0$, $x(\tau')=(\omega_0/c)X(t')$, and $\mathbf{g}$ is a slowly varying function ($|dg(\tau')/d\tau'|\ll 1$), which is trivially related to $\mathbf{a}$ as

$$\mathbf{g}[\tau'+x(\tau')]=\frac{-im_e c}{2e\sqrt{2\pi}}\mathbf{a}\{[ct'+X(t')]/c\tau_0\}. \tag{24}$$

Making use of Eq. (21) we rewrite Eq. (23) as

$$f_\pm=\pm\int_{-\infty}^{+\infty}g[\tau'+x(\tau')]\exp[i\tau'(-n\pm 1)+ix(\tau')(n\pm 1)]\times[1-x'(\tau')]d\tau'. \tag{25}$$

We wish to examine the integral (25) for very large n. For this purpose, we notice that the derivative of the phase

$$\Theta(\tau')=\tau'(-n\pm 1)+x(\tau')(n\pm 1) \tag{26}$$

is negative everywhere except in the vicinity of $\tau'_g=\omega_0 t'_g$ for which $x'(\tau'_g)\approx 1$ [see Fig. 4(a)].

The physical meaning of τ'_g and the behavior of $x(\tau')$ in the vicinity of these times is explained by Eq. (10). Since the time derivative of $\Theta(\tau')$ is negative for all τs that are not too close to one of the τ'_gs, we can shift the path over which we integrate to the lower half of the complex plane everywhere except in the neighborhood of τ'_g [see Fig. 4(b)]. The contributions of the parts remote from the real axis are exponentially small. We can shift the path to the complex plane until the derivative equals zero or we find a singularity of the phase Θ.

To calculate the contributions of τ'_g neighborhoods we can expand $x'(\tau')$ near each of its maxima at τ'_g. Since every smooth function resembles a parabola near its extrema, the

expansion of $x'(\tau')$ is a quadratic function of $(\tau'-\tau'_g)$. Simple integration leads to the following expression for $x(\tau')$:

$$x(\tau') = x(\tau'_g) + v_0(\tau'_g)(\tau'-\tau'_g) - \frac{\alpha(\tau'_g)}{3}(\tau'-\tau'_g)^3. \quad (27)$$

The Taylor expansion given by Eq. (27) has three important properties related to its dependence on S and a_0: (1) for S =const and $a_0 \to +\infty$ one finds that $v_0 \to c$; (2) for $a_0 \to +\infty$, α depends only on the parameter S; (3) the expansion (27) is a good approximation for $|\tau'-\tau'_g| \ll (2\pi/\omega_0) f_1(S)$, where the function f_1 does not depend on a_0. These three properties are mathematical statements of the physical picture described in Sec. II combined with the similarity theory developed in Sec. III. In other words, the properties of the expansion (27) just mentioned are direct consequences of the physical picture presented in Fig. 2.

The substitution of Eq. (27) into $f_{\pm}(n)$ yields

$$f_{\pm}(n) = \sum_{\tau'_g} f_{\pm}(\tau'_g, n), \quad (28)$$

where the sum is over all times τ'_g,

$$f_+(\tau'_g, n) = g[\tau'_g + x(\tau'_g)]\exp[i\Theta_+(\tau'_g, n)]F(\tau'_g, n), \quad (29)$$

$$f_-(\tau'_g, n) = -g[\tau'_g + x(\tau'_g)]\exp[i\Theta_-(\tau'_g, n)]F(\tau'_g, -n), \quad (30)$$

$$F(\tau'_g, n) = \frac{4\sqrt{\pi}}{[\sqrt[4]{\alpha(\tau'_g)}n]^{4/3}} \mathrm{Ai}\left(\frac{2}{n_{cr}(\tau'_g)} \frac{n - n_{cr}(\tau'_g)}{[\alpha(\tau'_g)n]^{1/3}}\right), \quad (31)$$

$$\Theta_{\pm} = \pm[\tau'_g + x(\tau'_g)] + n[x(\tau'_g) - \tau'_g], \quad (32)$$

and $n_{cr} = 2/(1-v_0)$. In Eq. (31) Ai is the well-known Airy function, defined as

$$\mathrm{Ai}(x) = \frac{1}{\sqrt{\pi}} \int_0^{+\infty} \cos\left(ux + \frac{1}{3}u^3\right) du. \quad (33)$$

Note that if $x(\tau'+\pi) = x(\tau')$ and $g(\tau') = g(\tau'+\pi)$, then $f_{\pm}(2n) = 0$. Using Eqs. (28)–(32) we can show analytically that the spectrum of radiation generated by the plasma is described by a universal formula.

For the intensity of the nth harmonic we obtain

$$I_n \propto |\exp[i\Theta_+(n)]F(n) - \exp[i\Theta_-(n)]F(-n)|^2, \quad (34)$$

where

$$F(n) = \frac{4\sqrt{\pi}}{(\sqrt[4]{\alpha}n)^{4/3}} \mathrm{Ai}\left(\frac{2}{n_{cr}} \frac{n - n_{cr}}{(\alpha n)^{1/3}}\right), \quad (35)$$

$$\Theta_{\pm}(n) = \pm\Theta_0 - n\Theta_1, \quad (36)$$

with the Airy function $\mathrm{Ai}(x)$ defined in Eq. (33) and the critical harmonic number n_{cr} satisfying $n_{cr} = 4\gamma_{\max}^2$, where $\gamma_{\max}$ is the largest relativistic factor of the plasma boundary.

Equation (34) gives an exact formula for the high-order harmonic spectrum, which includes both power law and exponential decay parts. Now we want to use different asymptotic representations of the Airy function in order to demonstrate explicitly these two quite different laws of high-order harmonic intensity decay.

For $n < \sqrt{\alpha/8} n_{cr}^{3/2}$ $[2|1 - n/n_{cr}| \ll (\alpha n)^{1/3}]$ we can substitute the value of the Airy function at $x=0$ $[\mathrm{Ai}(0) = \sqrt{\pi}/[3^{2/3}\Gamma(2/3)] = 0.629$, $\mathrm{Ai}'(0) = -3^{1/6}\Gamma(2/3)/(2\sqrt{\pi}) = -0.459]$ in Eq. (34), and obtain

$$I_n \propto \frac{1}{n^{8/3}} \left| \sin\Theta_0 + \frac{\mathrm{Ai}'(0)}{\mathrm{Ai}(0)} B(n, \Theta_0) \right|^2, \quad (37)$$

where

$$B(n, \Theta_0) = \frac{2\sin\Theta_0}{(\alpha n_{cr})^{1/3}} \left(\frac{n}{n_{cr}}\right)^{2/3} + \frac{2i\cos\Theta_0}{(\alpha n)^{1/3}}. \quad (38)$$

This means that the universal spectrum

$$I_n \propto 1/n^{8/3} \quad (39)$$

is observed everywhere except for $\sin\Theta_0 \approx 0$, when the dominant term in the expansion is zero. For this particular case, a higher-order correction is important for

$$(\alpha n)^{1/3} \tan\Theta_0 < 2 \left| \frac{\mathrm{Ai}'(0)}{\mathrm{Ai}(0)} \right| \quad (40)$$

and in this restricted frequency range the spectrum

$$I_n \propto 1/n^{10/3} \quad (41)$$

should be used.

At this point we want to explain the meaning of 8/3-spectrum universality. Notice that since Eq. (37) depends on the phase Θ, for moderate values of n_{cr} the best power-law fit of the high-order harmonic spectrum can be delivered by

$$I_n \propto n^{-p}, \quad (42)$$

where $8/3 \leqslant p \leqslant 10/3$. When n_{cr} becomes really large, the majority of the harmonics does not satisfy the inequality (40) and the spectrum inevitably becomes $I_n \propto n^{-8/3}$. In other words, one should think of the 8/3 spectrum as the high-intensity limit of the high-order harmonic spectrum. To find an analytical criterion for the 8/3-spectrum generation one can state that the condition (40) has to be violated for the harmonics with $n \propto \sqrt{\alpha/8} n_{cr}^{3/2}$. This means that

$$\gamma_{\max} > \gamma_{8/3} = \frac{1}{\sqrt{2}\tan\Theta_0} \left| \frac{\mathrm{Ai}'(0)}{\mathrm{Ai}(0)} \right|. \quad (43)$$

The formal expansion of the Airy function for

$$n \ll n_{cr}, \quad (\alpha n)^{1/3} < 1 \quad (44)$$

leads to the spectrum $I_n \propto 1/n^{5/2}$ discussed in Ref. [1]. However, the similarity theory shows that α does not depend on a_0 and N_e separately, but on S, giving $\alpha = \alpha(S)$, whereas the cutoff is $\propto a_0^3$. Moreover for experimental laser-overdense plasma interaction S is of the order of unity, therefore one expects $\alpha \approx 1$. As a result an increase in a_0 (S=const) leads to the violation of condition (44) for all but the lowest harmonics. This makes the case of $I_n \propto n^{-5/2}$ irrelevant. How-

ever, the analytically accurate spectrum $I_n \propto n^{-p}$ with the exponent $p=2.67$ differs from the one with $p=2.5$ predicted in Ref. [1] only by 0.17. This difference is hardly distiguishable numerically and experimentally. What does differ is the actual cutoff of the spectrum. The approximation presented in Ref. [1] delivers a cutoff located at $n_{cr}=4\gamma_{\max}^2$. Our present analysis shows that although the spectrum begins to deviate from the exact power law at n_{cr}, this deviation is small and can be neglected. The significant cutoff begins only at $n \propto \sqrt{\alpha/8}n_{cr}^{3/2} \propto \gamma_{\max}^3$ and therefore is parametrically larger than n_{cr}. This new result opens a way to important applications.

For $n > \sqrt{\alpha/8}n_{cr}^{3/2}$ $[2|1-n/n_{cr}| \gg (\alpha n)^{1/3}]$ Eq. (31) can be rewritten as

$$I_n \propto \frac{n_{cr}^{1/2}}{n^3} \exp\left(-\frac{16\sqrt{2}}{3\alpha^{1/2}}\frac{n-n_{cr}}{n_{cr}^{3/2}}\right). \tag{45}$$

It is interesting to notice that the approximation used in Ref. [1] also gives Eq. (45) for this area.

VI. ULTRASHORT PULSE DURATION

For ultrashort pulse generation not only the amplitudes but also the harmonic phases are of importance. The calculations presented above show that all harmonics are phase locked. This means that after proper filtering they can produce a pulse of duration T, such that

$$T \propto \frac{\pi}{\omega_0}\frac{1}{\sqrt{\alpha}n_{cr}^{3/2}} \propto \frac{1}{\sqrt{\alpha}\gamma_{\max}^3}, \tag{46}$$

where ω is the frequency of the fundamental wave.

Equation (46) presents a new result. Notice that the plasma boundary never moves with a relativistic γ factor larger than $\gamma_{\max}$. Consequently, the frequency of a photon reflected from this boundary due to the relativistic Doppler effect does not exceed $4\gamma_{\max}^2\omega_0=n_{cr}\omega_0$. How can a pulse with duration T given by Eq. (46) be produced then?

Mathematically this can be understood looking at the properties of the Airy function. $\mathrm{Ai}(x)$ changes its behavior from oscillatory for $x<0$ with $|x| \gg 1$,

$$\mathrm{Ai}(x) \approx \frac{1}{|x|^{1/4}} \sin\left(\frac{2}{3}|x|^{3/2}+\frac{\pi}{4}\right), \tag{47}$$

to exponentially decaying for $x \gg 1$,

$$\mathrm{Ai}(x) \approx \frac{1}{2x^{1/4}} \exp\left(-\frac{2}{3}x^{3/2}\right). \tag{48}$$

The point $x=0$ corresponds to $n=n_{cr}$. However, the exponential is so small for $n<\sqrt{\alpha/8}n_{cr}^{3/2}$ that the power-law decay dominates over the exponent. As a result, the power-law spectrum goes well beyond the threshold $\omega_0 n_{cr}$ predicted by oversimplified models considering reflection from a moving surface.

The reasoning just presented explains the mathematical origin of the $\sqrt{\alpha/8}n_{cr}^{3/2}$ cutoff. In the next section we give a simple physical interpretation of this result and reveal its relation to the relativistic γ-factor spikes. We also take a closer look at the mathematical origin of the cutoff.

VII. RELATIVISTIC SPIKES AND CUTOFF OF THE HIGH-ORDER HARMONIC SPECTRUM

The γ^3 scaling of the spectrum cutoff (1) is readily understood using the relativistic γ-factor spikes of the plasma-surface motion. Indeed, the plasma-surface velocity in the vicinity of a maximum can be approximated as

$$v(t) = v_0(t_g) - \alpha\omega_0^2(t-t_g)^2 \tag{49}$$

(see Sec. V). Consequently, for the surface γ factor during a relativistic spike we find

$$\gamma(t) \approx \frac{\gamma_{\max}}{\sqrt{1+\gamma_{\max}^2\alpha\omega_0^2(t-t_g)^2}}, \tag{50}$$

where $\gamma_{\max}=1/\sqrt{1-v_0^2(t_g)/c^2}$. Equation (50) shows that the highest-order harmonics are generated over the time interval

$$\Delta t \propto \frac{1}{\omega_0}\frac{1}{\sqrt{\alpha}\gamma_{\max}}. \tag{51}$$

For the whole time interval Δt the relativistic spike moves with ultrarelativistic velocity in the direction of the emitted radiation. For this reason, the spatial length L of the high-order harmonic pulse produced is

$$L \propto [c-v_0(t_g)]\Delta t \propto \frac{c}{\omega_0}\frac{1}{\sqrt{\alpha}\gamma_{\max}}. \tag{52}$$

A pulse of such duration contains frequencies

$$\Omega \propto \frac{c}{L} \propto \omega_0\sqrt{\alpha}\gamma_{\max}^3, \tag{53}$$

which physically explains the origin of the high-frequency cutoff (1). This cutoff should be compared with the one predicted by the oscillating mirror model $4\gamma_{\max}^2$. It differs parametrically from the correct cutoff $\propto\sqrt{8\alpha}\gamma_{\max}^3$, which is due to the relativistic γ-factor spikes.

As it has been shown, the oscillating mirror model gives the incorrect formula for the spectrum cutoff because it does not include the relativistic γ-factor spikes. Mathematically, this failure of the oscillating mirror model [10,18] is related to the saddle-point overlapping. Equation (26) defines the saddle points

$$\frac{dx(\tau')}{d\tau'} = 1 \pm \frac{1}{n}, \tag{54}$$

the vicinity of which determines the value of the integral describing the amplitude of the nth harmonic, $n \gg 1$ (see Fig. 4). Equation (27) yields that the set of Eq. (54) has real (not imaginary) solutions only for $n<n_{cr}=4\gamma_{\max}^2$. For larger n all of the saddle points of Eq. (54) have an imaginary part.

Let us now apply the standard saddle-point method to the problem without investigating whether the conditions for its applicability are met (it is clear that these conditions are violated at least for $n \approx n_{cr}$, for which two saddle points coincide). This approximation predicts that for $1 \ll n \ll n_{cr}$, the spectrum decays as $1/n^{5/2}$. For $n>n_{cr}$, this approach restores Eq. (48).

As was mentioned above, the spectrum $1/n^{5/2}$ occurs formally in the limit $(\alpha n)^{1/3}<1$. In other words, if α were small, this spectrum would be observed. However, since α depends on S rather than a_0, this spectrum corresponds to harmonics with small numbers only and is hardly of any practical interest. On the other hand, one can notice that α describes the plasma-surface acceleration at the maximum of the velocity. This means that the limit of small α (and the spectrum $1/n^{5/2}$) describes the limit of the surface moving without acceleration. However, this limit is of little interest for large a_0.

VIII. CUTOFF AND THE STRUCTURE OF FILTERED PULSES

As we have seen, the relativistic plasma harmonics are phase locked and can be used to generate ultrashort pulses. However, to extract these ultrashort pulses, one has to remove the lower harmonics. The high-energy cutoff (1) of the power-law spectrum defines the shortest pulse duration that can be achieved this way.

Let us apply a high-frequency filter that suppresses all harmonics with frequencies below Ω_f and study how the relative position of the Ω_f and the spectrum cutoff affects the duration of the resulting (sub)attosecond pulses.

According to Eq. (34), the electric field of the pulse after the filtration is

$$E \propto \mathrm{Re}\int_{\Omega_f/\omega_0}^{+\infty} \{\exp[i\Theta_+(n)]F(n) - \exp[i\Theta_-(n)]F(-n)\}\exp(int)dn. \tag{55}$$

The structure of the filtered pulses depends on where we set the filter threshold Ω_f. In the case $1 \ll \Omega_f/\omega_0 \ll \sqrt{\alpha/8}n_{cr}^{3/2}$, we use Eq. (39) and rewrite Eq. (55) as

$$E \propto \mathrm{Re}\int_{\Omega_f/\omega_0}^{+\infty} \frac{\exp(int)}{n^{4/3}}dn = \left(\frac{\omega_0}{\Omega_f}\right)^{1/3} \mathrm{Re}\exp(i\Omega_f t - i\Theta_1)P(\Omega_f t), \tag{56}$$

where the function P

$$P(x) = \int_1^{+\infty} \frac{\exp(iyx)}{y^{4/3}}dy \tag{57}$$

gives the slow envelope of the pulse.

It follows from the expression (56) that the electric field of the filtered pulse decreases very slowly with the filter threshold as $\Omega_f^{-1/3}$. The pulse duration decreases as $1/\Omega_f$. At the same time, the fundamental frequency of the pulse is Ω_f. Therefore the pulse is hollow when $\Omega_f/\omega_0 \ll \sqrt{8\alpha}\gamma_{\max}^3$, i.e., its envelope is not filled with electric-field oscillations. One possible application of these pulses is to study atom excitation by means of a single strong kick.

The pulses structure changes differ significantly when the filter threshold is placed above the spectrum cutoff. For $\Omega_f/\omega_0 \gg \sqrt{8\alpha}\gamma_{\max}^3$ we use Eqs. (45) and (55) to obtain

$$E \propto \left(\frac{\omega_0}{\Omega_f}\right)^{3/2} \exp\left(-\frac{8\sqrt{2}\Omega_f}{3\sqrt{\alpha}\omega_0 n_{cr}^{3/2}}\right)\mathrm{Re}\frac{\exp(i\Omega_f t - i\Theta_1)}{8\sqrt{2}/(3\sqrt{\alpha}n_{cr}^{3/2}) + i\omega_0 t}. \tag{58}$$

Th amplitude of these pulses decreases fast when Ω_f grows. However, the pulse duration $\propto 1/\sqrt{\alpha}\gamma_{\max}^3$ does not depend on Ω_f. Since the fundamental frequency of the pulse grows as Ω_f, the pulses obtained with an above-cutoff filter are filled with electric-field oscillations. Therefore these pulses are suitable to study the resonance excitation of ion and atom levels.

The minimal duration of the pulse obtained by cutting off low-order harmonics is defined by the spectrum cutoff $\propto\sqrt{\alpha 8}\gamma_{\max}^3$. Physically, this result is the consequence of the ultrarelativistic spikes in the plasma-surface γ factor.

IX. SPECTRUM MODULATIONS

In this section we discuss the harmonic phases and show how the interference of harmonics produced by different γ spikes can lead to spectrum modulations.

Equation (28) obtained in Sec. V allows for straightforward physical interpretation. The sum $f_-(\tau_g',n)+f_+(\tau_g',n)$ gives the contribution of the τ_g' spike of the surface-relativistic factor to the harmonic spectrum (see Fig. 4). Therefore the phase of the nth harmonic ϕ_n due to the τ_g' spike is given by

$$\tan[\phi_n(\tau_g') + n\Theta_1(\tau_g')]\tan(\Theta_0) = \frac{1 - F(\tau_g',-n)/F(\tau_g',n)}{1 + F(\tau_g',-n)/F(\tau_g',n)}, \tag{59}$$

where $\Theta_0(\tau_g')=\tau_g'+x(\tau_g')$ is the phase of the incident laser pulse at the time τ_g' and $\Theta_1(\tau_g')=\tau_g'-x(\tau_g')=\tau(\tau_g')$, the time of the observation, i.e., the symbol Θ_1 is redundant, yet we keep it for the sake of notation coherency.

Since $F(\tau_g',-n)\approx F(\tau_g',n)$ for $n\gg 1$, Eq. (59) gives rise to $\phi_n(\tau_g')\approx -n\Theta_1(\tau_g')$. This means that each spike radiates phase-locked high-order harmonics that can be used for ultrashort pulse production. Another consequence of $F(\tau_g',-n)\approx F(\tau_g',n)$ is that the amplitude of the harmonics is proportional to $\sin[\Theta_0(\tau_g')]$.

The mechanism presented in Fig. 2 has another very interesting consequence. Each harmonic is generated due to several spikes. These spikes contribute to Eq. (28) with different phase multipliers. This phase difference leads to modulations in the high-order harmonic spectrum. As an example we consider the interference between the harmonics produced by two different spikes in detail. The phase shift between the contributions from different spikes is

$$\phi_n(\tau_{g_1}') - \phi_n(\tau_{g_2}') = \Theta_0(\tau_{g_1}') - \Theta_0(\tau_{g_2}') - n[\Theta_1(\tau_{g_1}') - \Theta_1(\tau_{g_2}')]$$

and can be large for large n. Since for

$$n \ll \min[\sqrt{\alpha(\tau'_{g_1})/8}n_{cr}^{3/2}(\tau'_{g_1}), \sqrt{\alpha(\tau'_{g_2})/8}n_{cr}^{3/2}(\tau'_{g_2})]$$

only Ai(0) enters $f_{\pm}(\tau'_{g_{1,2}})$, the values of the contributions from the $\tau'_{g_{1,2}}$ spikes for this harmonic range do not depend on $n_{cr}(\tau'_{g_{1,2}})$. As a result the modulations in this harmonic range depend only on the parameter S. To recapitulate, the nontrivial plasma motion producing more than one γ spike per oscillation period is the cause of the spectrum modulation.

X. NUMERICAL RESULTS

In order to check our analytical results, we have performed a number of 1D PIC simulations with the 1D particle-in-cell code VLPL [24]. In all simulations a laser pulse with the Gaussian envelope $a=a_0\exp(-t^2/\tau_L^2)\cos(\omega_0 t)$, duration $\omega_0\tau_L=4\pi$, and dimensionless vector potential $a_0=20$ was incident onto a plasma layer with a step-density profile.

A. Apparent reflection point

First, we study the oscillatory motion of the plasma and the dynamics of the apparent reflection point defined by the boundary condition (16) [26]. The plasma slab is initially positioned between $x_R=-1.5\lambda$ and $x_L=-3.9\lambda$, where $\lambda=2\pi/\omega_0$ is the laser wavelength. The laser pulse has the amplitude $a_0=20$. The plasma density is $N_e/N_c=90$ ($S=4.5$).

At every time step, the incident and the reflected fields are recorded at $x=0$ (the position of the "external observer"). Being solutions of the wave equation in vacuum, these fields can be easily chased to arbitrary x and t. To find the ARP position x_{ARP}, we solve numerically Eq. (18). The trajectory of $x_{\mathrm{ARP}}(t)$ obtained in this simulation is presented in Fig. 5(a). One can clearly see the oscillatory motion of the point $x_{\mathrm{ARP}}(t)$. The equilibrium position is displaced from the initial plasma-boundary position x_R due to the mean laser-light pressure.

Since only the ARP motion towards the laser pulse is of importance for the HHG, we cut out the negative ARP velocities $v_{\mathrm{ARP}}(t)=dx_{\mathrm{ARP}}(t)/dt$ and calculate only the positive ones [Fig. 5(b)]. The corresponding γ factor $\gamma_{\mathrm{ARP}}(t)=1/\sqrt{1-v_{\mathrm{ARP}}(t)^2/c^2}$ is presented in Fig. 5(c). Notice that the ARP velocity is a smooth function. At the same time, the γ factor $\gamma_{\mathrm{ARP}}(t)$ contains sharp spikes, which coincide with the velocity extrema. These numerical results confirm the predictions of the ultrarelativistic similarity theory, which were presented in Sec. III.

B. High-order harmonic spectrum

For the same laser-plasma parameters ($a_0=20$, $N_e=90N_c$) the spectrum of high-order harmonic radiation is presented in Fig. 6. The maximum γ factor of the apparent reflection point in this numerical simulation is $\gamma_{\max}\approx 3.3$ (compare with Fig. 5). Consequently, the maximal harmonic number predicted by the oscillating mirror model lies at $4\gamma_{\max}^2\approx 40$, while the harmonic cutoff predicted by the relativistic spikes

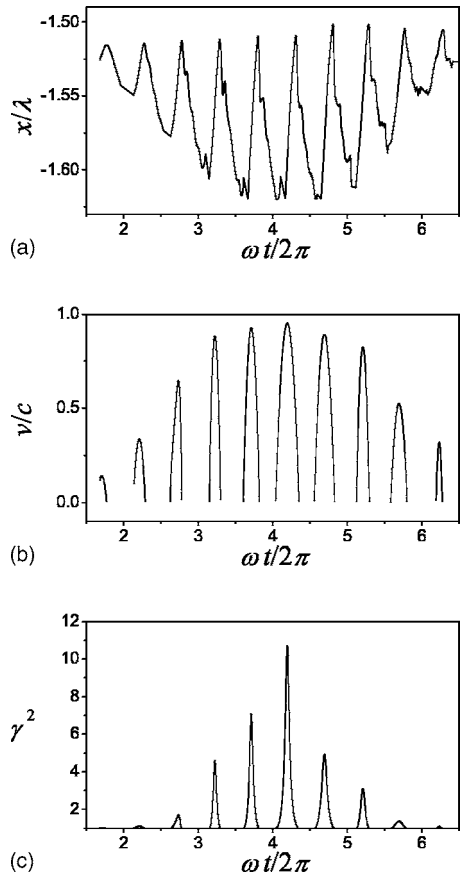

FIG. 5. 1D PIC simulation results for the parameters $a_0=20$ and $N_e=90N_c$. (a) Oscillatory motion of the point $x_{\mathrm{ARP}}(t)$ where $\mathbf{E}_\tau[x(t)]=0$. (b) Velocity $v_{\mathrm{ARP}}(t)=dx_{\mathrm{ARP}}(t)/dt$; only the positive velocities are shown, since they correspond to motion towards the laser pulse in the geometry of this simulation. Notice that the ARP velocity is a smooth function. (c) The corresponding γ factor $\gamma_{\mathrm{ARP}}(t)=1/\sqrt{1-v_{\mathrm{ARP}}(t)^2/c^2}$ contains sharp spikes, which coincide with the velocity extrema.

is about 100. Figure 6 clearly demonstrates that there is no change of the spectrum behavior at $4\gamma_{\max}^2$, while steeper decay takes place above 100, as predicted by our theory. Also, the spectral-intensity modulations discussed in Sec. V and Refs. [3,25] are observed.

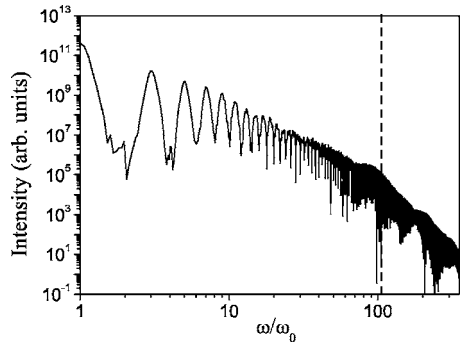

FIG. 6. Spectrum of high-order harmonics obtained numerically for the case of $a_0=20$ and $N_e=90N_c$, corresponding to $S=4.5$ and $\gamma_{\max}\approx 3.3$. Assuming $\alpha\approx 1$, the cutoff (1) is expected at $n\approx 100$. This analytically predicted cutoff is marked by the dashed line.

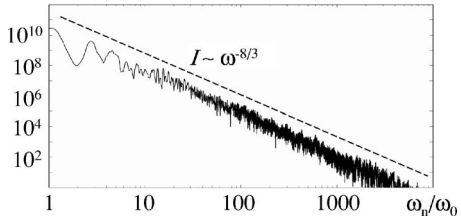

FIG. 7. Spectra of the reflected radiation for the laser amplitude $a_0=20$ and the plasma density $N_e=30N_{cr}$. The broken line marks the universal scaling $I \propto \omega^{-8/3}$.

To be able to make a real statement about the power in the power-law decay of the spectrum we need more harmonics in order to satisfy the condition of universal 8/3-spectrum formation (43). For this reason we made the simulation with parameters $a_0=20$ and $N_e=30N_c$, which roughly corresponds to solid hydrogen or liquid helium. The reflected radiation spectrum obtained for these parameters is shown in Fig. 7 in the log-log scale. The power-law spectrum $I_n \propto 1/n^{8/3}$ is clearly seen here, thus confirming the analytical results of Sec. V.

C. Subattosecond pulses

Let us take a closer look at Fig. 7. The power-law spectrum extends at least until the harmonic number 2000 and zeptosecond (1 zs$=10^{-21}$ s) pulses can be generated. The temporal profile of the reflected radiation is shown in Fig. 8. When no spectral filter is applied [Fig. 8(a)], a train of attosecond pulses is observed [18]. However, when we apply a spectral filter selecting harmonics above $n=300$, a train of much shorter pulses is obtained [Fig. 8(b)]. Figure 8(c) zooms into one of these pulses. Its full width at half maximum (FWHM) is about 300 zs. At the same time its intensity normalized to the laser frequency is huge $(eE_{zs}/mc\omega)^2 \approx 14$. This corresponds to the intensity $I_{zs} \approx 2 \times 10^{19}$ W/cm^2.

D. Filter threshold and the attosecond pulse structure

The dependence of the short pulses on the position of the filter also can be studied numerically. We apply a filter with the filter function $f(\omega)=1+\tanh[(\omega-\Omega_f)/\Delta\omega]$. It passes through frequencies above Ω_f and suppresses lower frequencies. We choose the similation case of laser-vector potential $a_0=20$ and plasma density $N_e=90N_c$. The spectrum of high-order harmonics is given in Fig. 6. We zoom into one of the pulses in the pulse train obtained and study how the shape of this one pulse changes with Ω_f. Figure 9 represents the pulse behavior for four different positions of Ω_f. We measure to what degree the pulse is filled by the number of field oscillations within the FWHM. One clearly sees that for filter threshold below the cutoff frequency [Figs. 9(a) and 9(b)], the pulse is hollow. Notice that the case of Fig. 9(b) corresponds to the cutoff frequency predicted by the oscillating mirror model. Only for filter threshold positions above the spectrum cutoff given by Eq. (1) the pulse becomes filled [Figs. 9(c) and 9(d)]. These results confirm once again the real position of the harmonic cutoff.

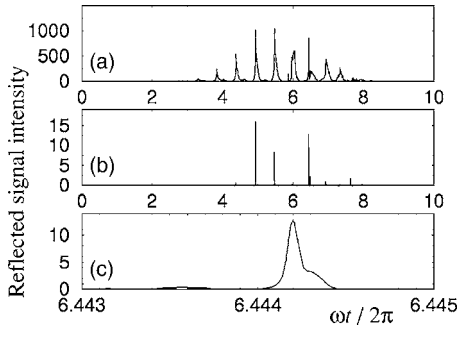

FIG. 8. Zeptosecond pulse train: (a) temporal structure of the reflected radiation; (b) zeptosecond pulse train seen after spectral filtering; and (c) one of the zeptosecond pulses zoomed (its FWHM duration is about 300 zs).

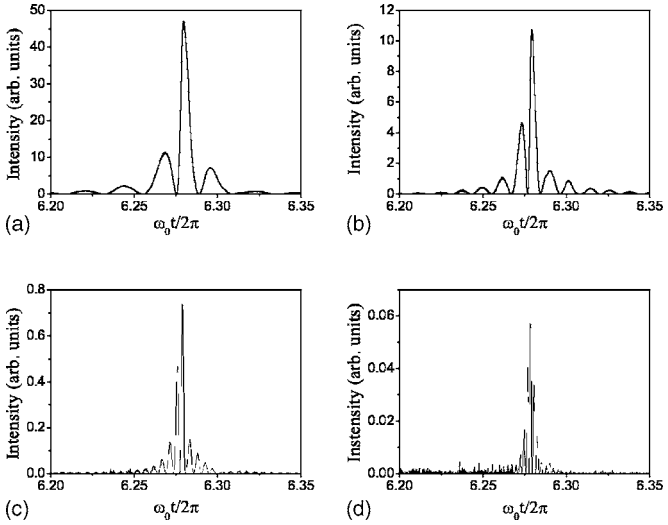

FIG. 9. Dependence of the pulse filling on the position of the sharp filter boundary for $a_0=20$ and $N_e=90N_c$ and filter positions: (a) $\Omega_f=20\omega_0$, $\Delta\omega=2\omega_0$; (b) $\Omega_f=40\omega_0$, $\Delta\omega=2\omega_0$; (c) $\Omega_f=100\omega_0$, $\Delta\omega=2\omega_0$; and (d) $\Omega_f=200\omega_0$, $\Delta\omega=2\omega_0$.

XI. DISCUSSIONS

In this work we have shown analytically and numerically that the relativistic γ-factor spikes are the physical cause for HHG at the boundary of overdense plasma. It is important that the properties of these spikes are universal and follow from the ultrarelativistic similarity theory. The universal physics of the relativistic γ spikes inheres in the universality of the high-order harmonic spectrum.

The spectrum of the high-order harmonics contains the power-law part $I_n \propto 1/n^{8/3}$, which goes until the cutoff at $\sqrt{8\alpha}\gamma_{\max}^3$. Here $\gamma_{\max}$ is the maximal γ factor and α describes the acceleration of the plasma boundary. This result demonstrates that a naive oscillating mirror model is insufficient for the correct treatment of HHG at plasma boundaries.

Physically and mathematically, the cutoff at $4\gamma_{\max}^2$ would correspond to a uniformly moving mirror without acceleration ($\alpha \to 0$ in our approach). In this case, the mirror upshifts the laser frequency when a full period of the laser radiation is reflected. In reality, however, only a short part of the laser

period is reflected (the γ-spike duration is $\tau_\gamma \propto 1/\gamma_{\max}\omega$). This leads to the broadening of the reflected radiation by the additional factor $\gamma_{\max}$ and to the much higher cutoff at $\propto \gamma_{\max}^3$.

ACKNOWLEDGMENTS

This work has been supported in part by DFG Transregio 18 and by DFG Graduierten Kolleg 1203.

[1] S. Gordienko, A. Pukhov, O. Shorokhov, and T. Baeva, Phys. Rev. Lett. **93**, 115002 (2004); **94**, 103903 (2005).
[2] G. D. Tsakiris, K. Eidmann, J. Meyer-ter-Vehn, and F. Krausz, New J. Phys. **8**, 19 (2006).
[3] I. Watts *et al.*, Phys. Rev. Lett. **88**, 155001 (2002).
[4] I. Watts *et al.*, Phys. Rev. E **66**, 036409 (2002).
[5] U. Wagner *et al.*, Phys. Rev. E **70**, 026401 (2004).
[6] B. Dromey, M. Zepf, A. Gopal *et al.*, Nat. Phys. **2**, 456 (2006).
[7] A. Pukhov, Nat. Phys. **2**, 439 (2006).
[8] R. L. Carman *et al.*, Phys. Rev. Lett. **46**, 29 (1981).
[9] B. Bezzerides *et al.*, Phys. Rev. Lett. **49**, 202 (1982).
[10] S. V. Bulanov *et al.*, Phys. Plasmas **1**, 745 (1993).
[11] P. Gibbon, Phys. Rev. Lett. **76**, 50 (1996).
[12] R. Lichters *et al.*, Phys. Plasmas **3**, 3425 (1996).
[13] D. von der Linde and K. Rzazewski, Appl. Phys. B: Lasers Opt. **63**, 499 (1996).
[14] R. Ondarza, Phys. Rev. E **67**, 066401 (2003).
[15] K. Eidmann *et al.*, Phys. Rev. E **72**, 036413 (2005).
[16] F. Krausz, Phys. World **14**, 41 (2001); M. Lewenstein, Science **297**, 1131 (2002); Ph. Bucksbaum, Nature (London) **421**, 593 (2003); N. A. Papadogiannis *et al.*, Phys. Rev. Lett. **83**, 4289 (1999); A. Pukhov, S. Gordienko, and T. Baeva, Phys. Rev. Lett. **91**, 173002 (2003).
[17] Y. I. Salamin, S. X. Su, and Ch. H. Keitel, Phys. Rep. **427**, 42 (2006).
[18] L. Plaja *et al.*, J. Opt. Soc. Am. B **7**, 1904 (1998).
[19] T. Baeva, Diploma thesis, 2005 (unpublished).
[20] J. D. Jackson, *Classical Electrodynamics* (Wiley, New York, 1999).
[21] S. Gordienko and A. Pukhov, Phys. Plasmas **12**, 043109 (2005).
[22] L. D. Landau, E. M. Lifshitz, and L. P. Pitaevskii, *Electrodynamics of Continuous Media* (Pergamon Press, Oxford, 1984).
[23] N. G. de Bruijn, *Asymptotic Methods in Analysis* (Dover, New York, 1981).
[24] A. Pukhov, J. Plasma Phys. **61**, 425 (1999).
[25] U. Teubner *et al.*, Phys. Rev. A **67**, 013816 (2003).
[26] T. Baeva *et al.*, e-print physics/0601044, Phys. Rev. Lett. (to be published).